Supporting Information

Formaldehyde Electrolysis in a Membrane-Free Electrolyzer: Low-Energy Hydrogen and Formate Co-Production with Cu-Based Boride Electrocatalysts

Sahil Thorawade[1], Rupali Patel[1], Aniruddha Bhide[1], Suraj Gupta[2], Rohan Fernandes[1], Nainesh Patel[1*]*

[1]Department of Physics and Electronics, Christ University, Bengaluru, 560029, India

[2]Advanced Materials Department, Jožef Stefan Institute, Jamova 39, 1000 Ljubljana, Slovenia

*Corresponding authors:

Prof. Nainesh Patel, Dr. Rupali Patel

E-mail:

nainesh.patel@christuniversity.in, rupali.patel@christuniversity.in

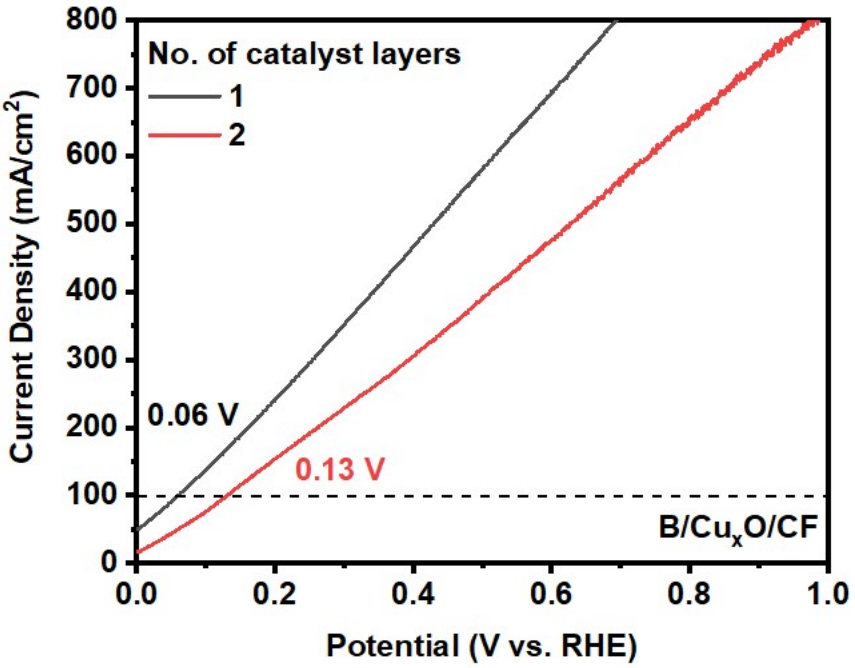

Fig. S1: Comparison of FOR activity for different catalyst loading

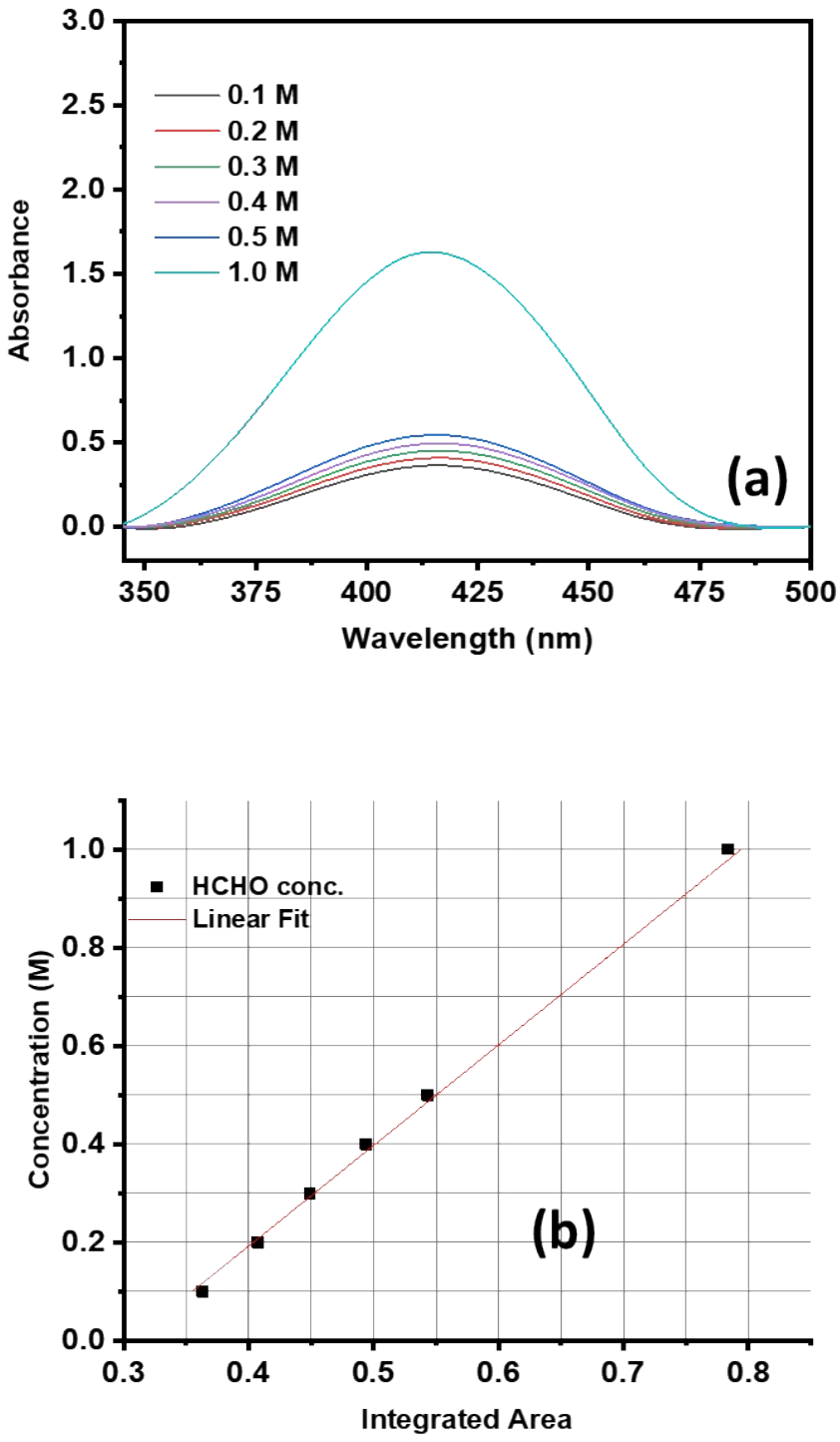

Fig. S2. (a) UV absorption spectra for known HCHO concentrations and (b) Calibration curve obtained using peak intensity of $\lambda = 413$ nm.

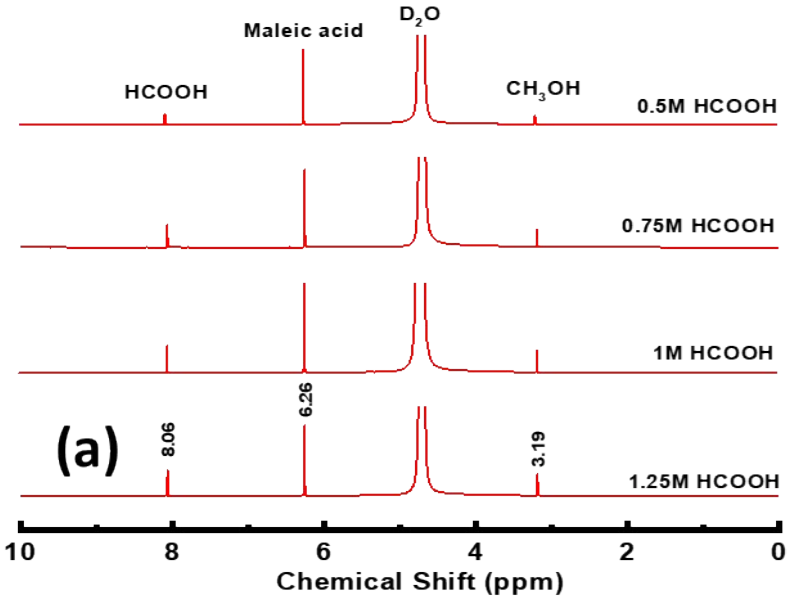
Maleic acid
D_2O
HCOOH
CH_3OH
0.5M HCOOH
0.75M HCOOH
1M HCOOH
1.25M HCOOH
(a)
8.06
6.26
3.19
10
8
6
4
2
0
Chemical Shift (ppm)

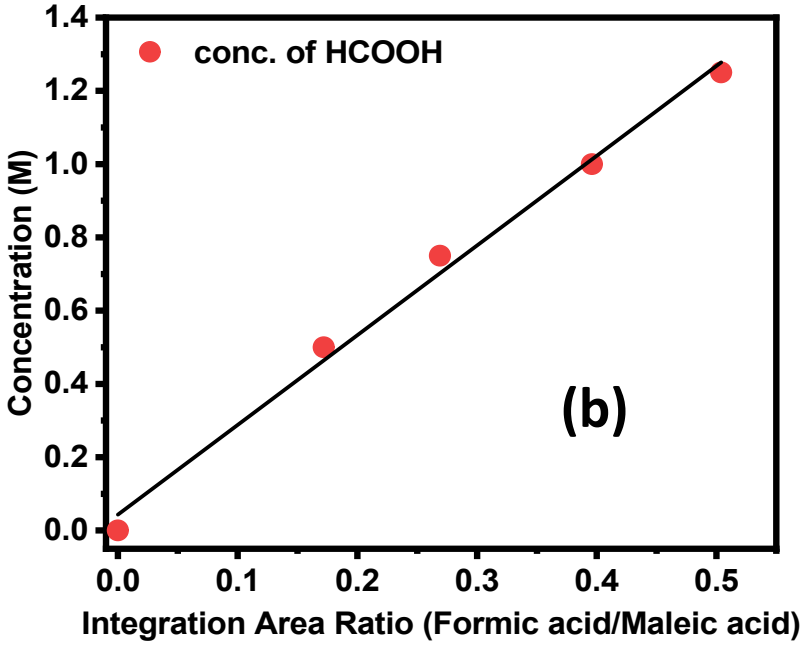
conc. of HCOOH
(b)
Concentration (M)
1.4
1.2
1.0
0.8
0.6
0.4
0.2
0.0
0.0
0.1
0.2
0.3
0.4
0.5
Integration Area Ratio (Formic acid/Maleic acid)

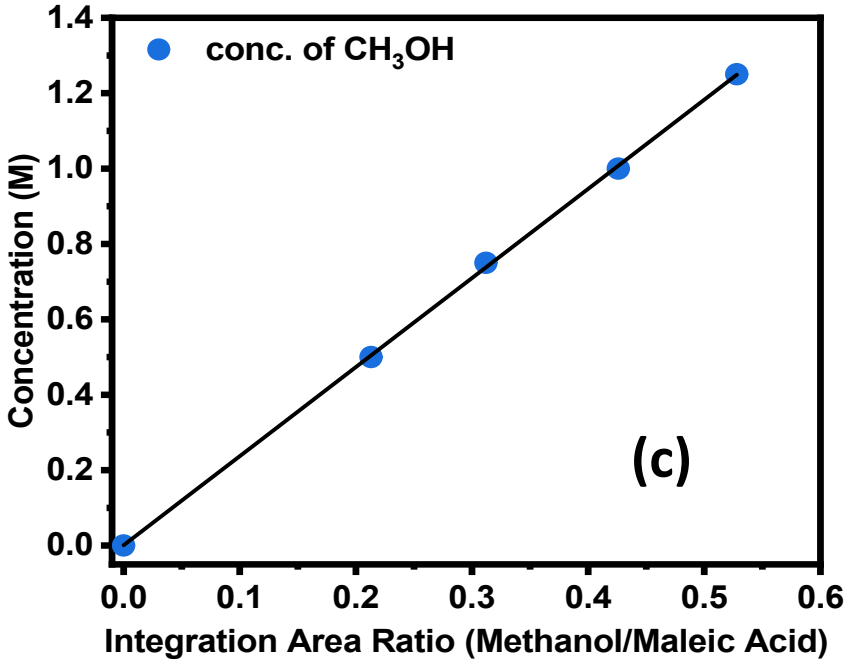

Fig. S3. (a) ^{1}H NMR spectra for a known concentration of HCOOH and Methanol; and Calibration curves obtained for (b) HCOOH and (c) Methanol.

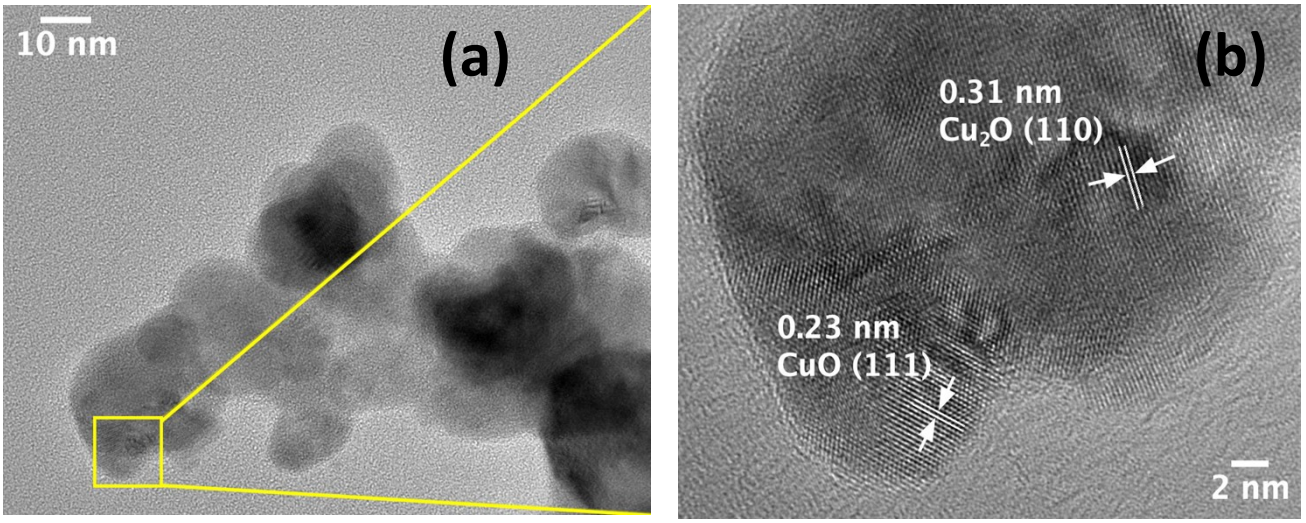

Fig. S4: (a) TEM and (b) HRTEM micrographs of B/Cu_xO/CF

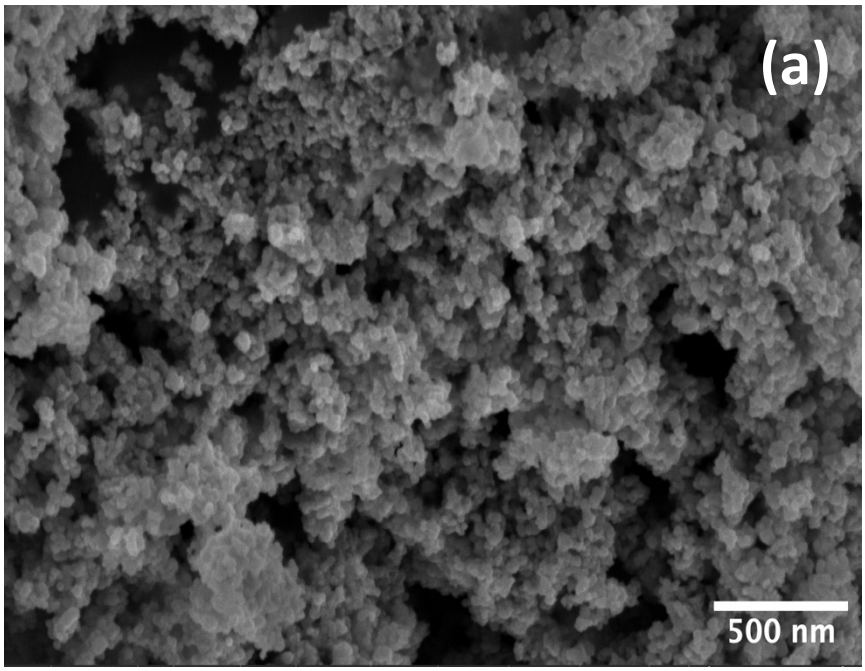

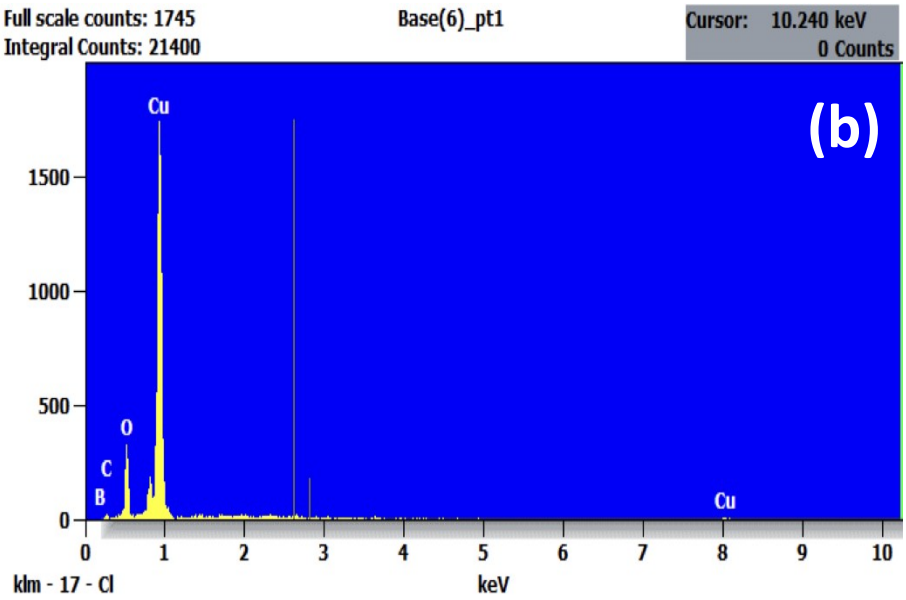

Element	B	C	O	Cu
Weight %	0	0.93	8.66	90.41

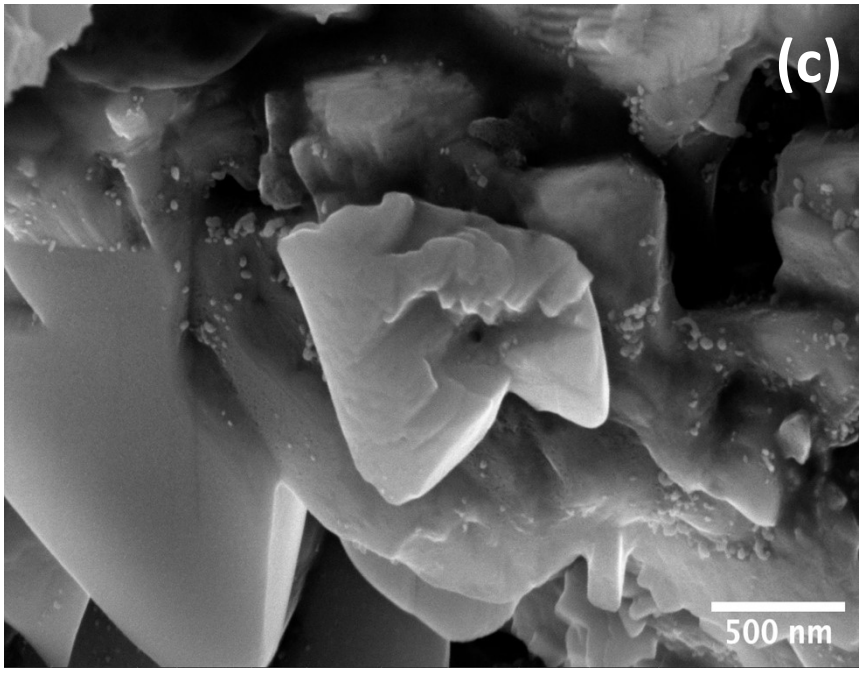

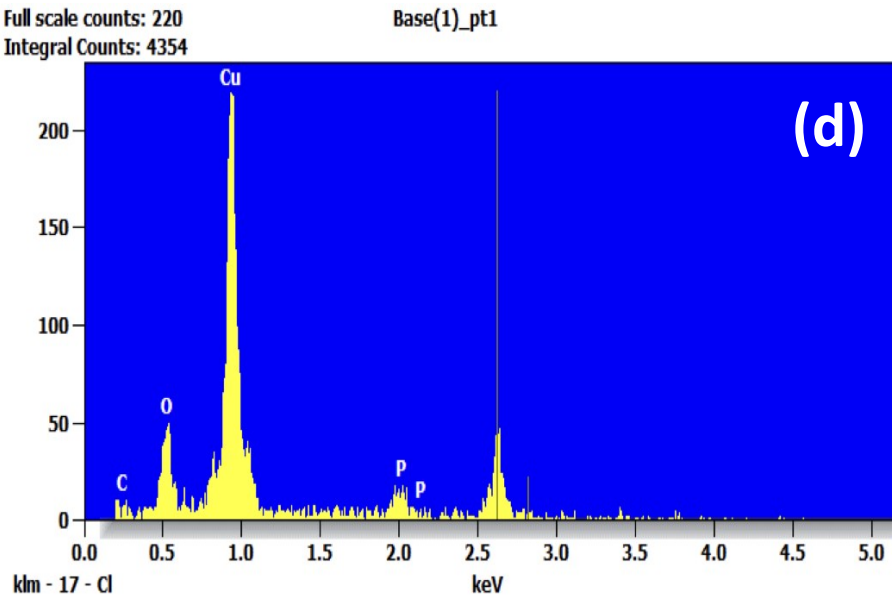

Element	P	C	O	Cu
Weight %	8.79	0.82	8.53	81.86

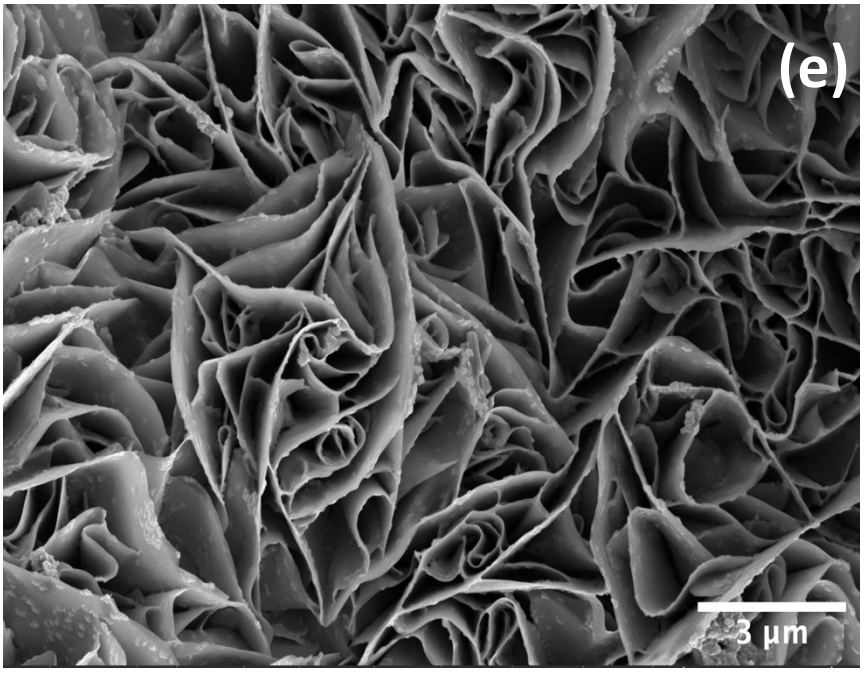

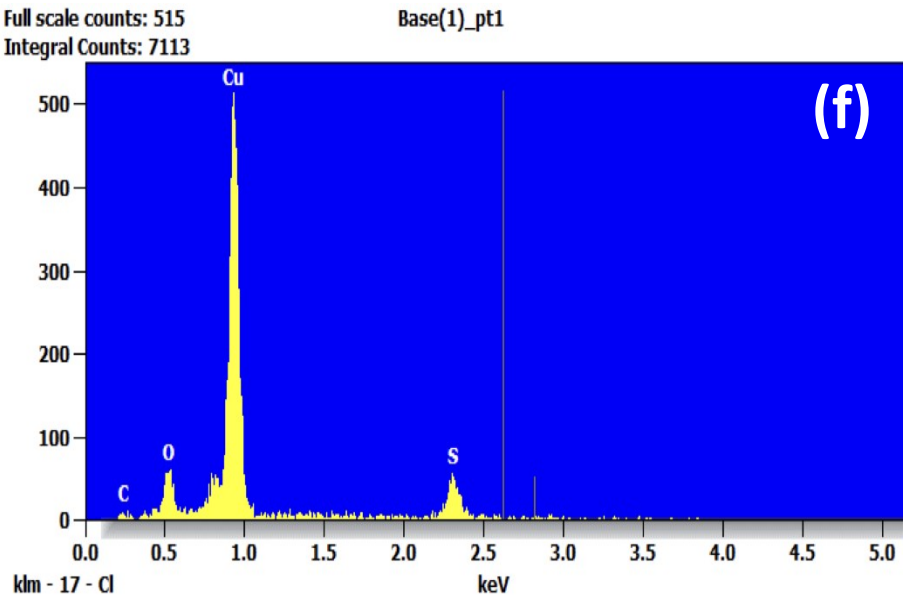

Element	S	C	O	Cu
Weight %	14.08	0.35	4.06	81.50

Fig. S5. SEM images of (a) B/Cu_xO/CF, (b) P/Cu_xO/CF, and (c) S/Cu_xO/CF, and (b, d, and f) corresponding EDS spectra.

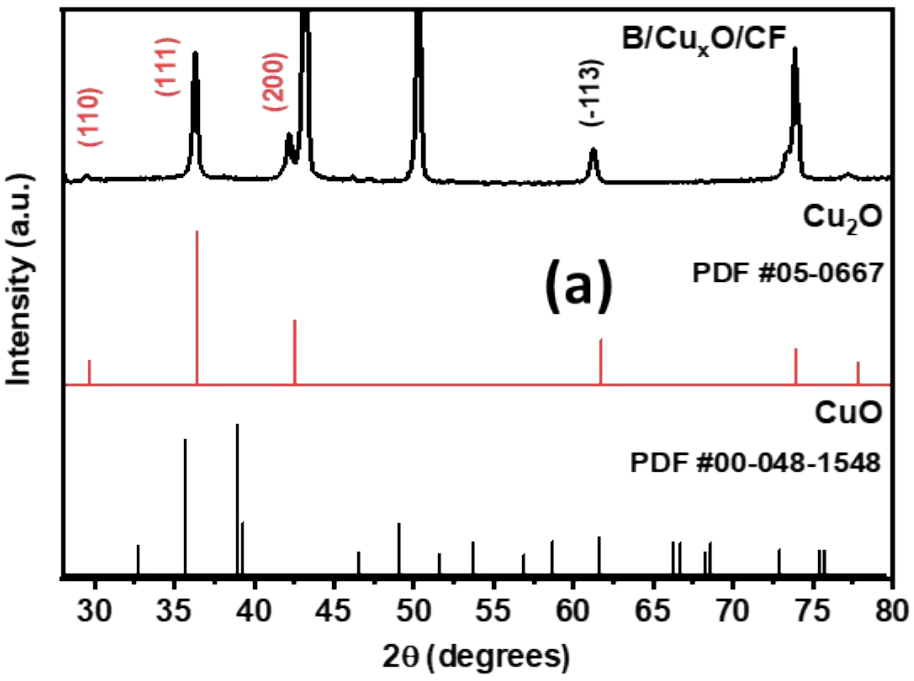
B/Cu$_x$O/CF
(110)
(111)
(200)
(-113)
Cu$_2$O
PDF #05-0667
(a)
CuO
PDF #00-048-1548
Intensity (a.u.)
30 35 40 45 50 55 60 65 70 75 80
2θ (degrees)

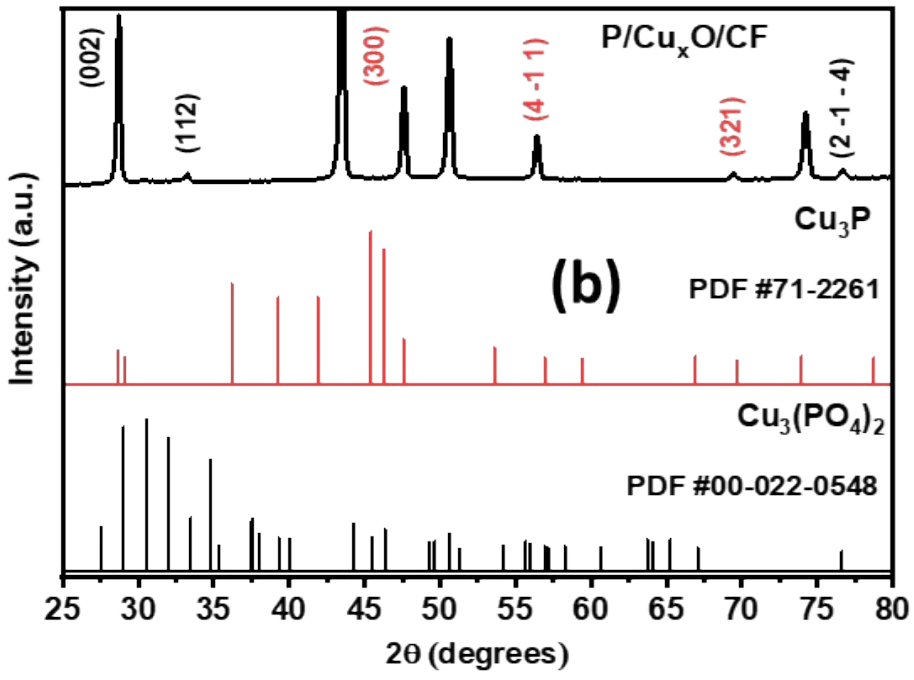
P/Cu$_x$O/CF
(002)
(112)
(300)
(4 -1 1)
(321)
(2 -1 - 4)
Cu$_3$P
PDF #71-2261
(b)
Cu$_3$(PO$_4$)$_2$
PDF #00-022-0548
Intensity (a.u.)
25 30 35 40 45 50 55 60 65 70 75 80
2θ (degrees)

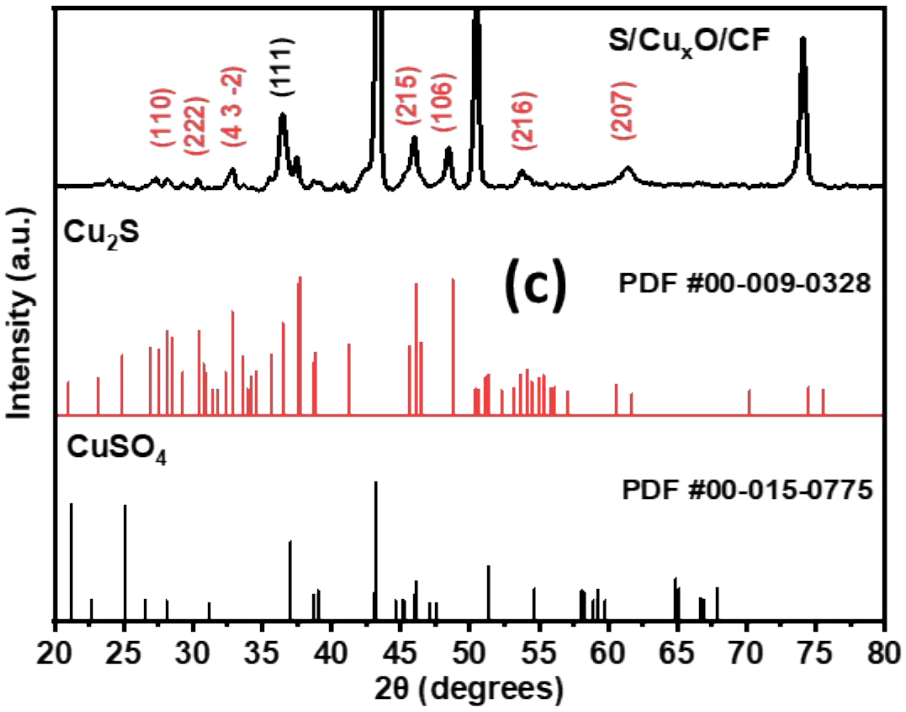

Fig. S6. XRD spectra of (a) B/Cu$_x$O/CF, (b) P/Cu$_x$O/CF, and (c) S/Cu$_x$O/CF electrocatalysts.

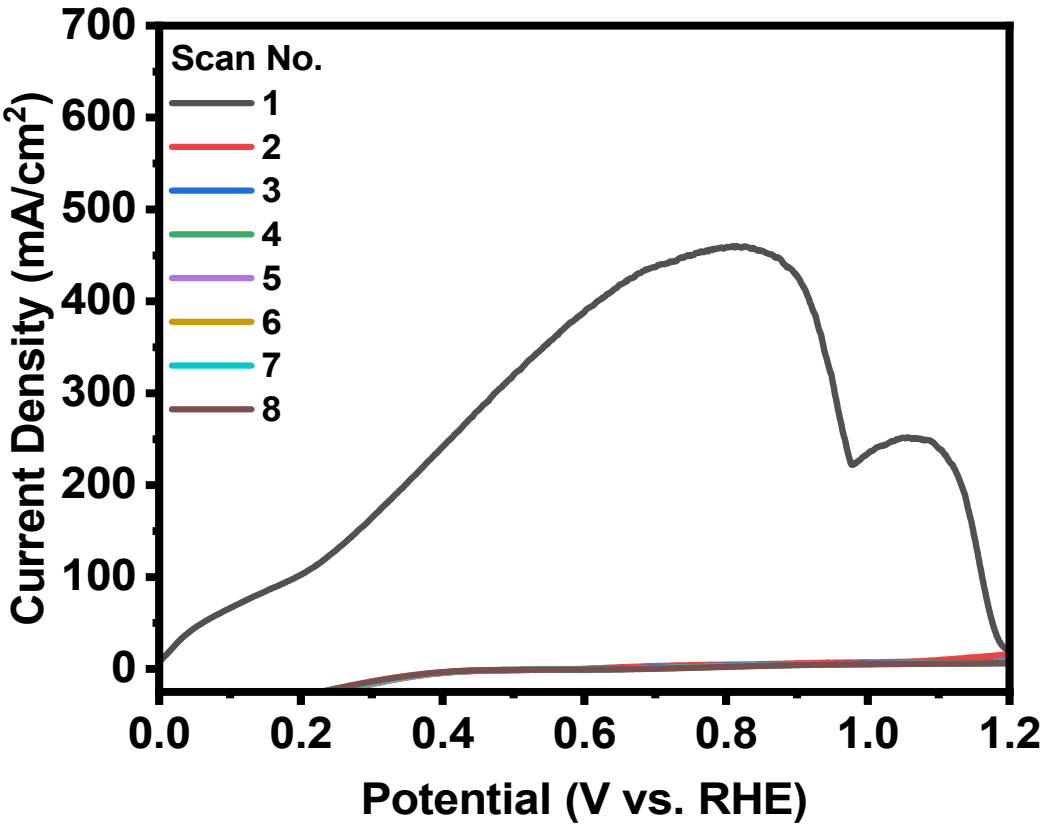

Fig. S7; Subsequent Linear Polarization Curves for FOR of P/Cu_xO/CF

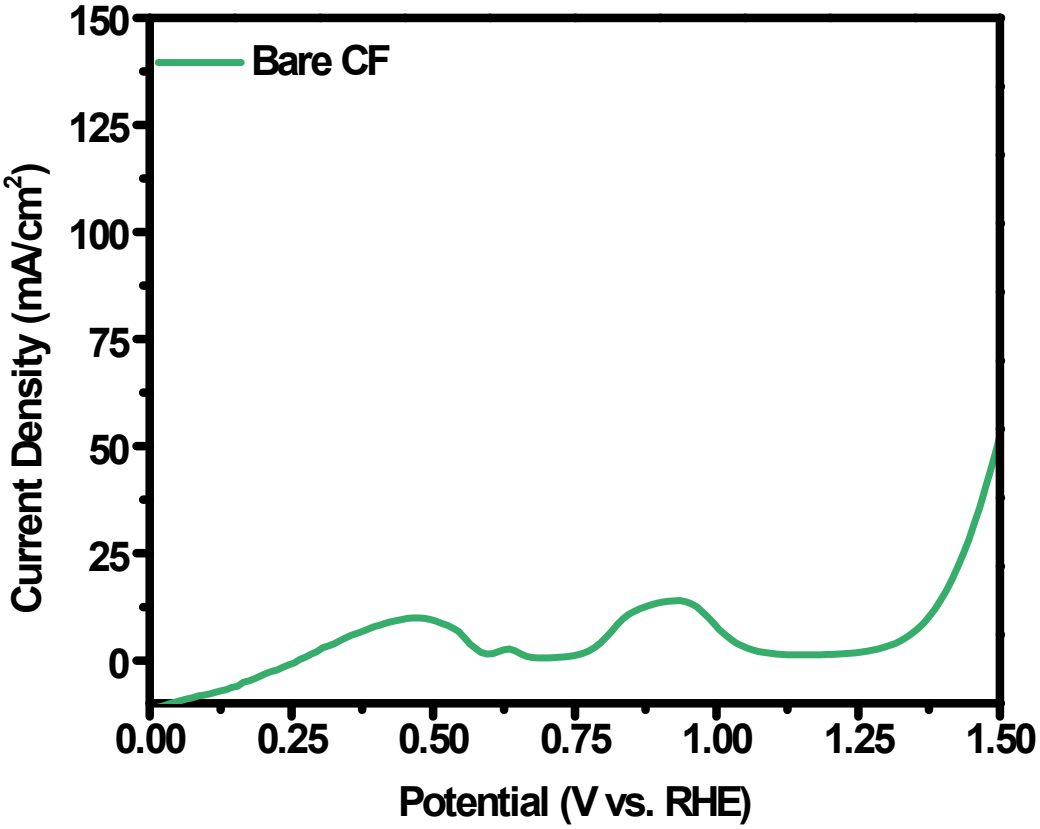

Fig. S8: Linear Polarization Curves for FOR of Cu foam.

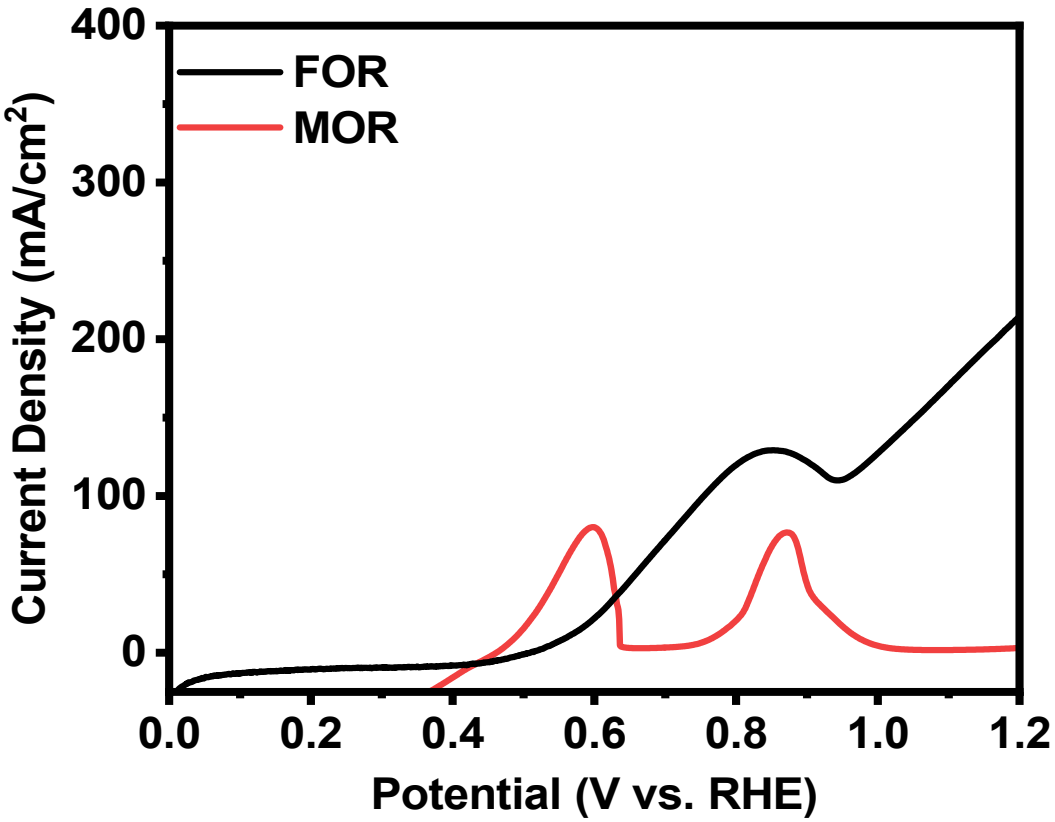

Fig. S9; Comparison of anodic activity for FOR and MOR of S/Cu_xO/CF catalyst.

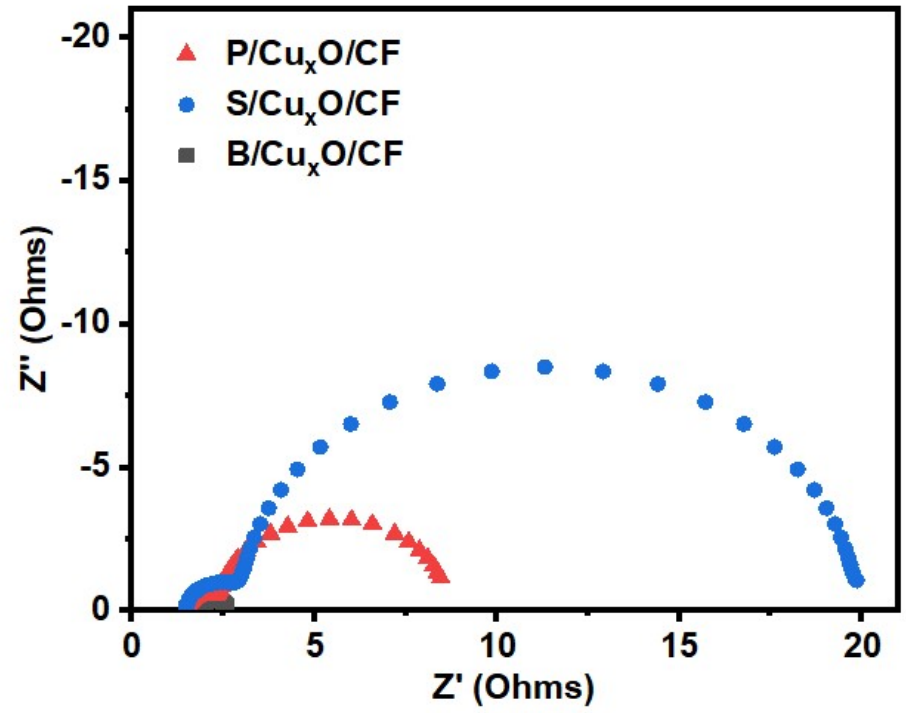

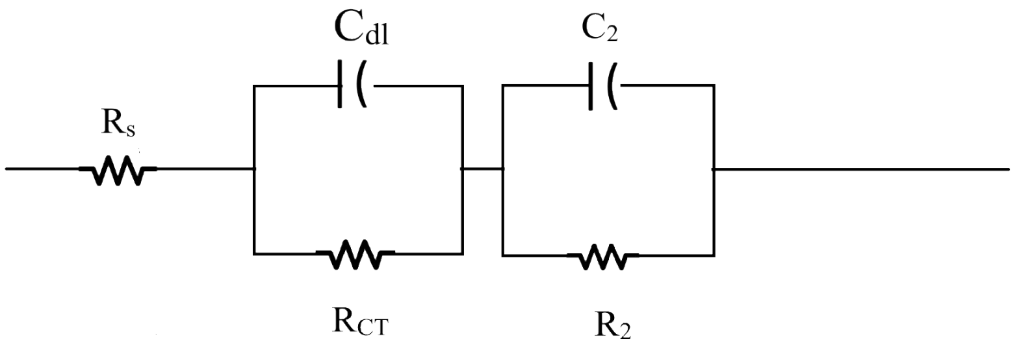

Fig. S10: EIS spectra for FOR of B, P, and S/Cu_xO/CF electrocatalysts and equivalent circuit for fitting and interpretation of data.

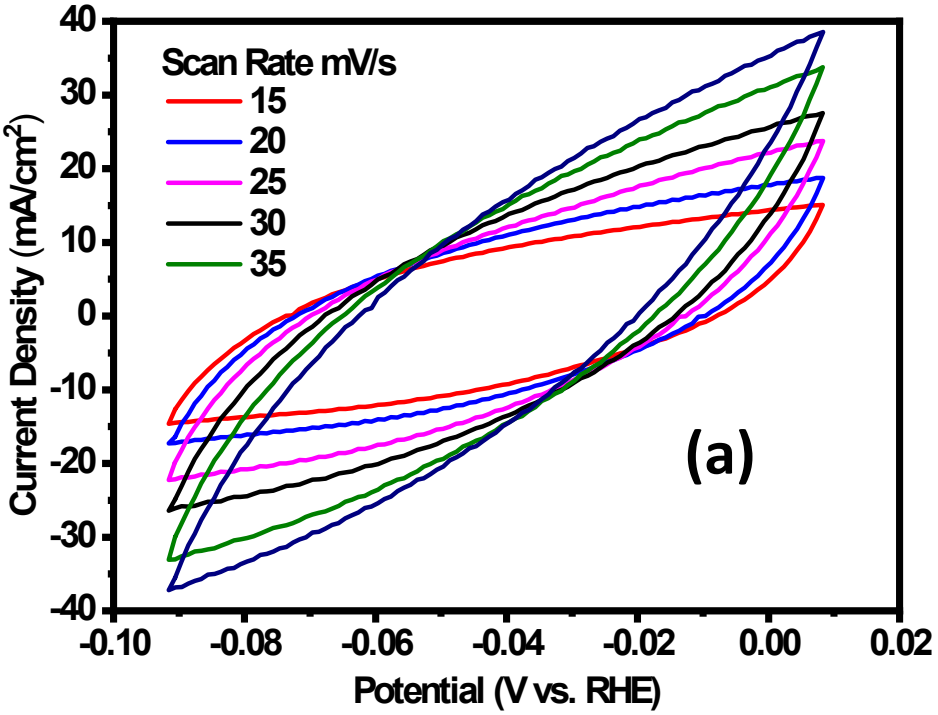
Scan Rate mV/s
15
20
25
30
35
(a)
Current Density (mA/cm^2)
Potential (V vs. RHE)
40
30
20
10
0
-10
-20
-30
-40
-0.10
-0.08
-0.06
-0.04
-0.02
0.00
0.02

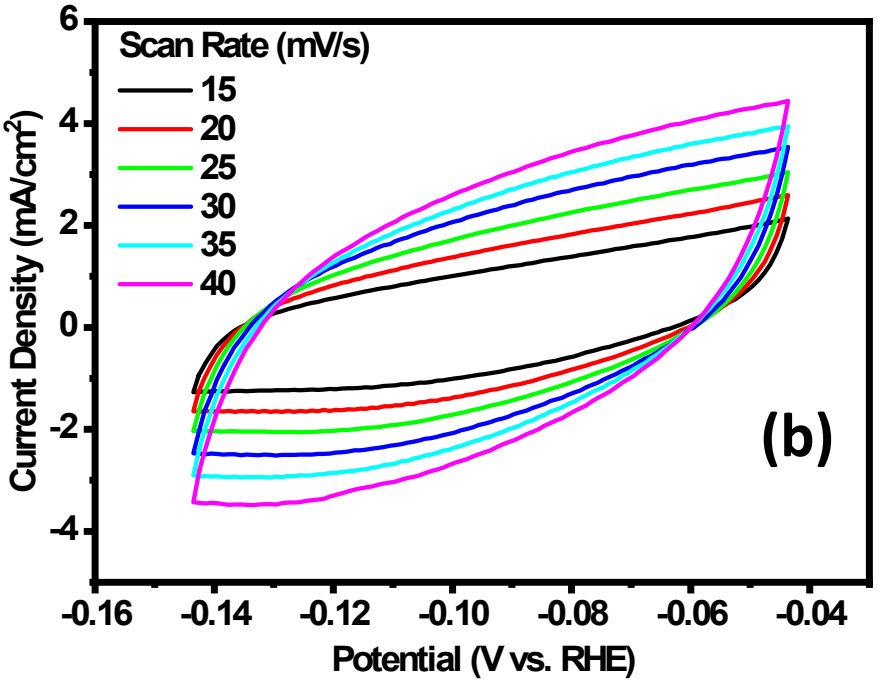
Scan Rate (mV/s)
15
20
25
30
35
40
(b)
Current Density (mA/cm^2)
Potential (V vs. RHE)
6
4
2
0
-2
-4
-0.16
-0.14
-0.12
-0.10
-0.08
-0.06
-0.04

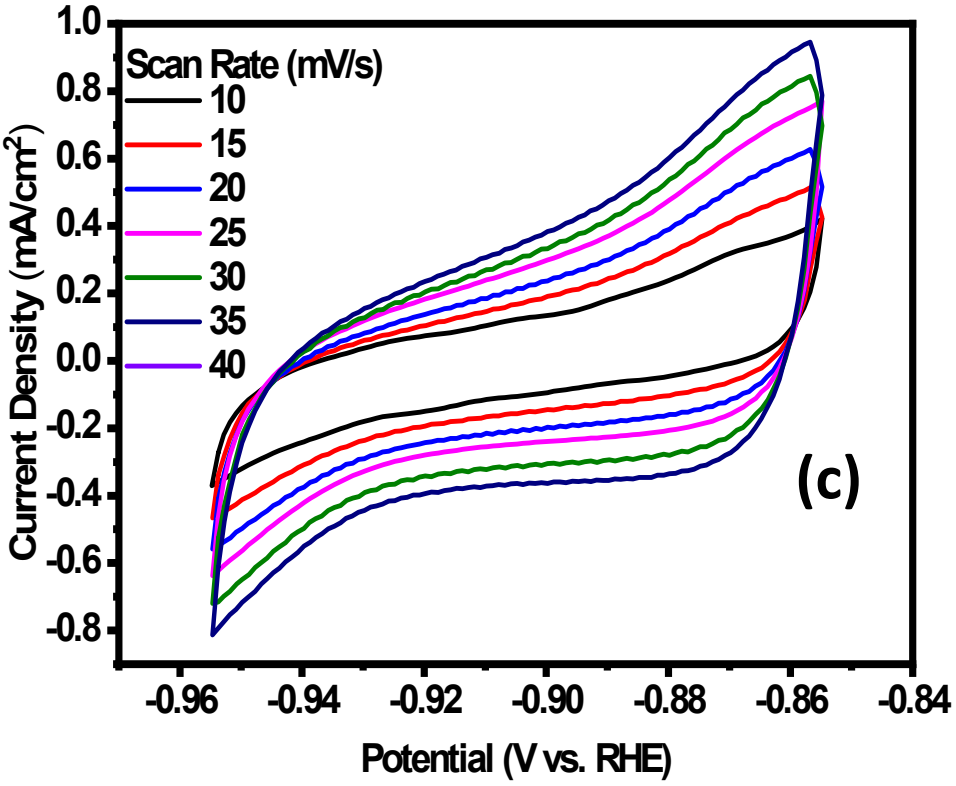

Fig. S11: Cyclic voltammetry curves for (a) B/Cu_xO/CF, (b) P/Cu_xO/CF, and (c) S/Cu_xO/CF electrocatalysts.

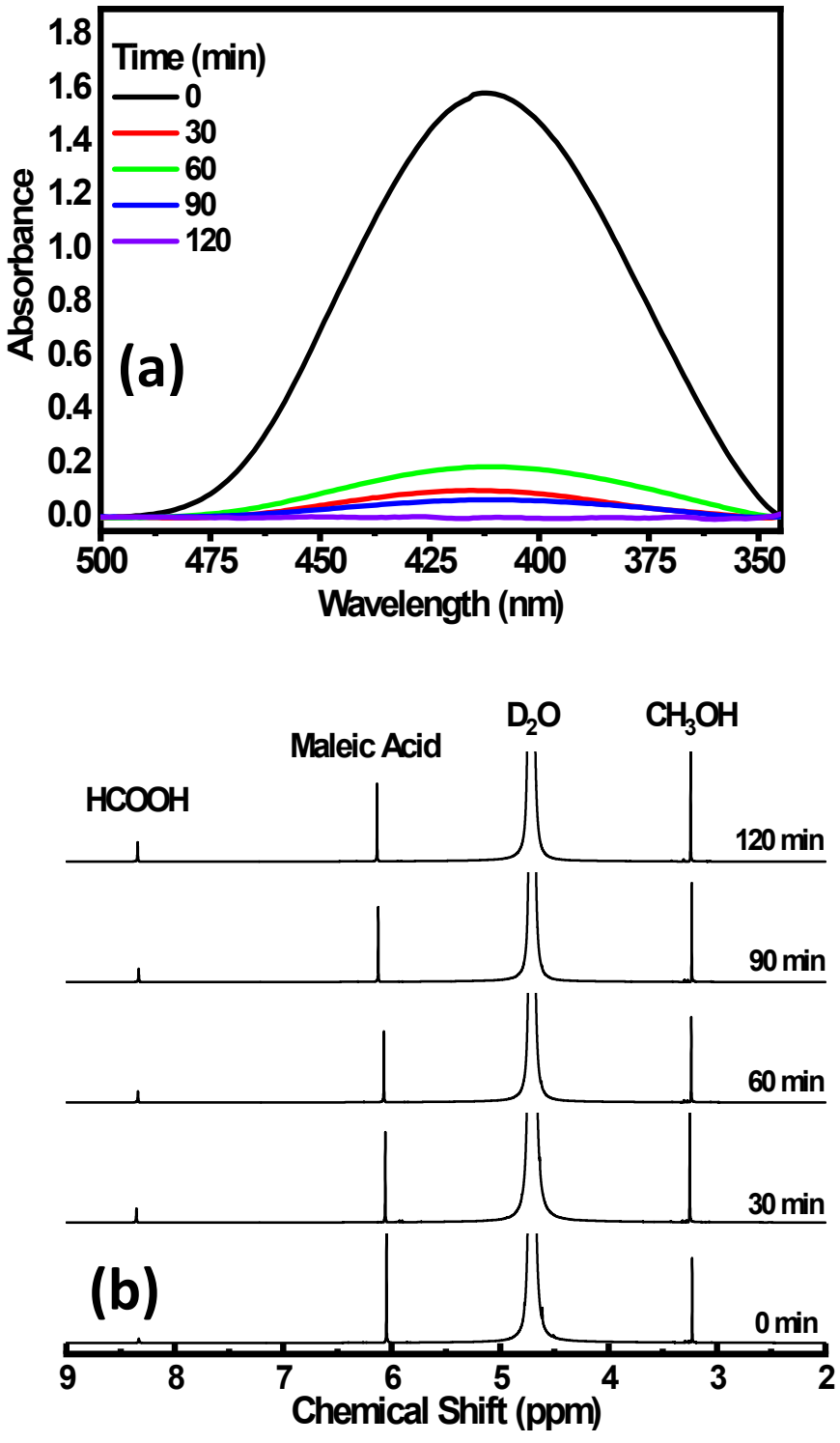

Fig. S12 (a): UV-Vis spectroscopy and (b) ^{1}H NMR spectroscopy at simultaneous periodic intervals during electrolysis test.

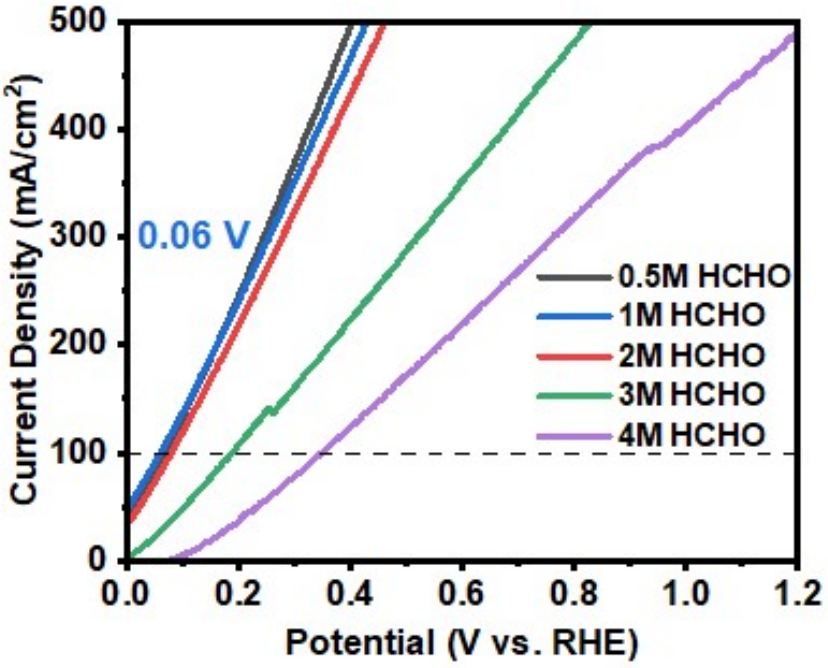

Fig. S13; FOR activity of B/Cu_xO/CF for different HCHO concentrations.

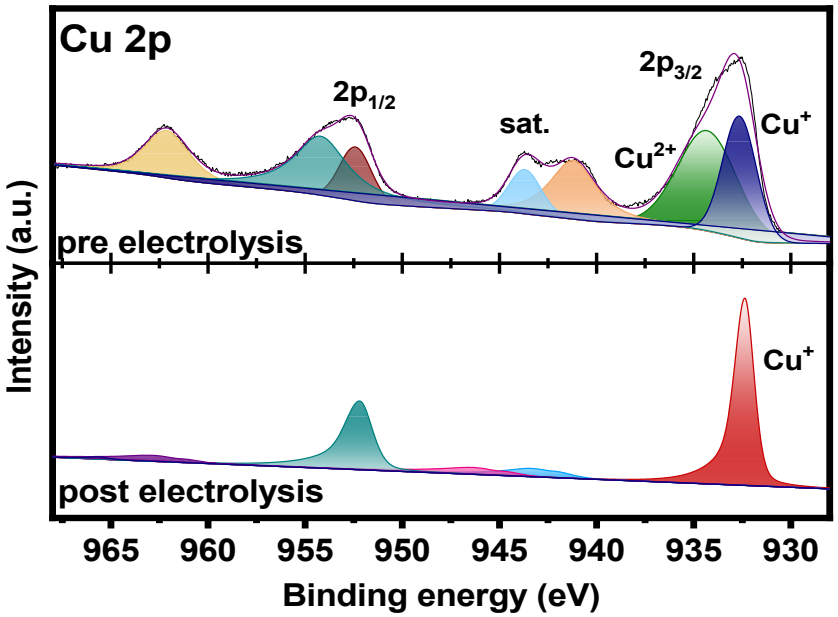

Fig. S14: Pre and Post FOR XPS spectra of B/Cu_xO/CF electrocatalyst

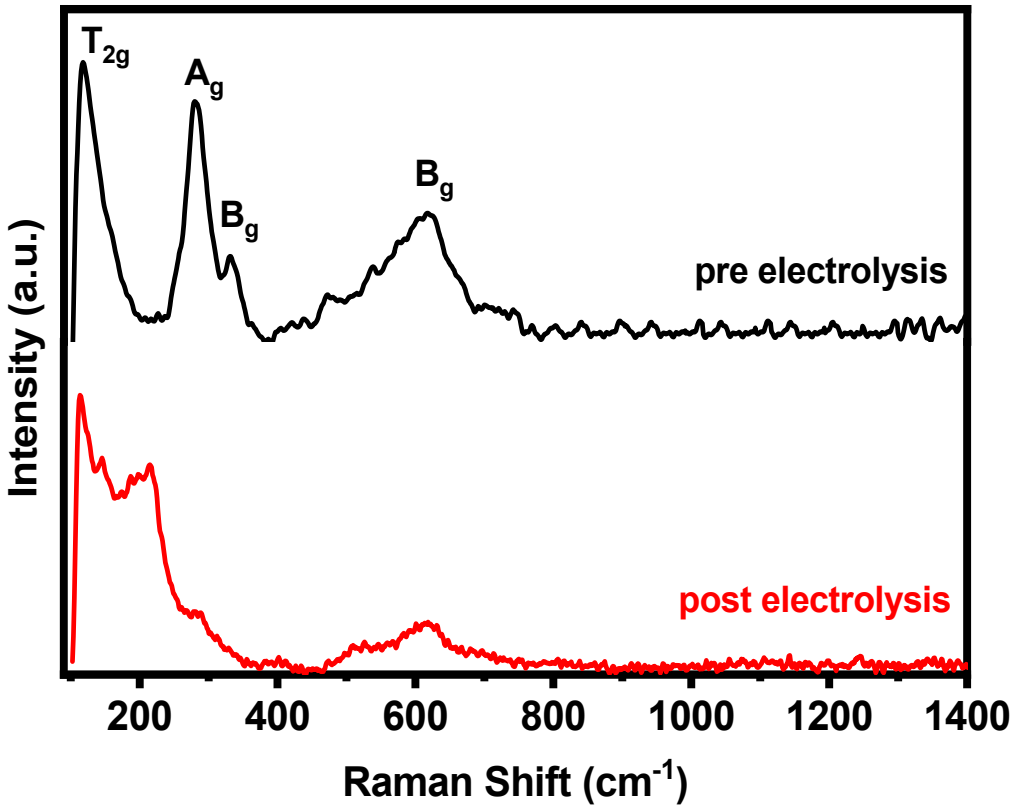

Fig. S15: Pre and Post FOR Raman spectra of B/Cu_xO/CF electrocatalyst.

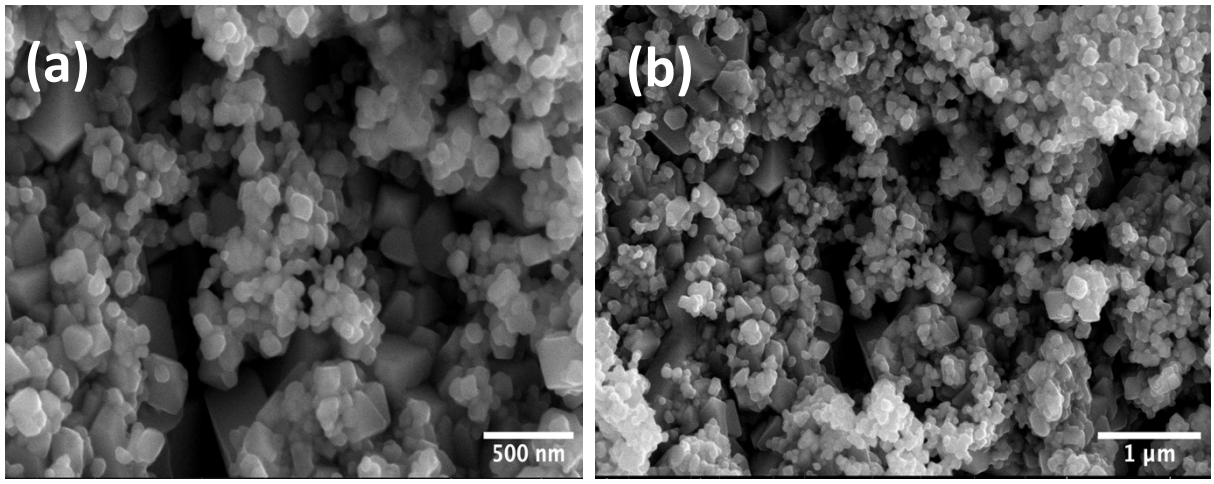

Fig. S16: Post FOR SEM images of B/Cu_xO/CF electrocatalyst.

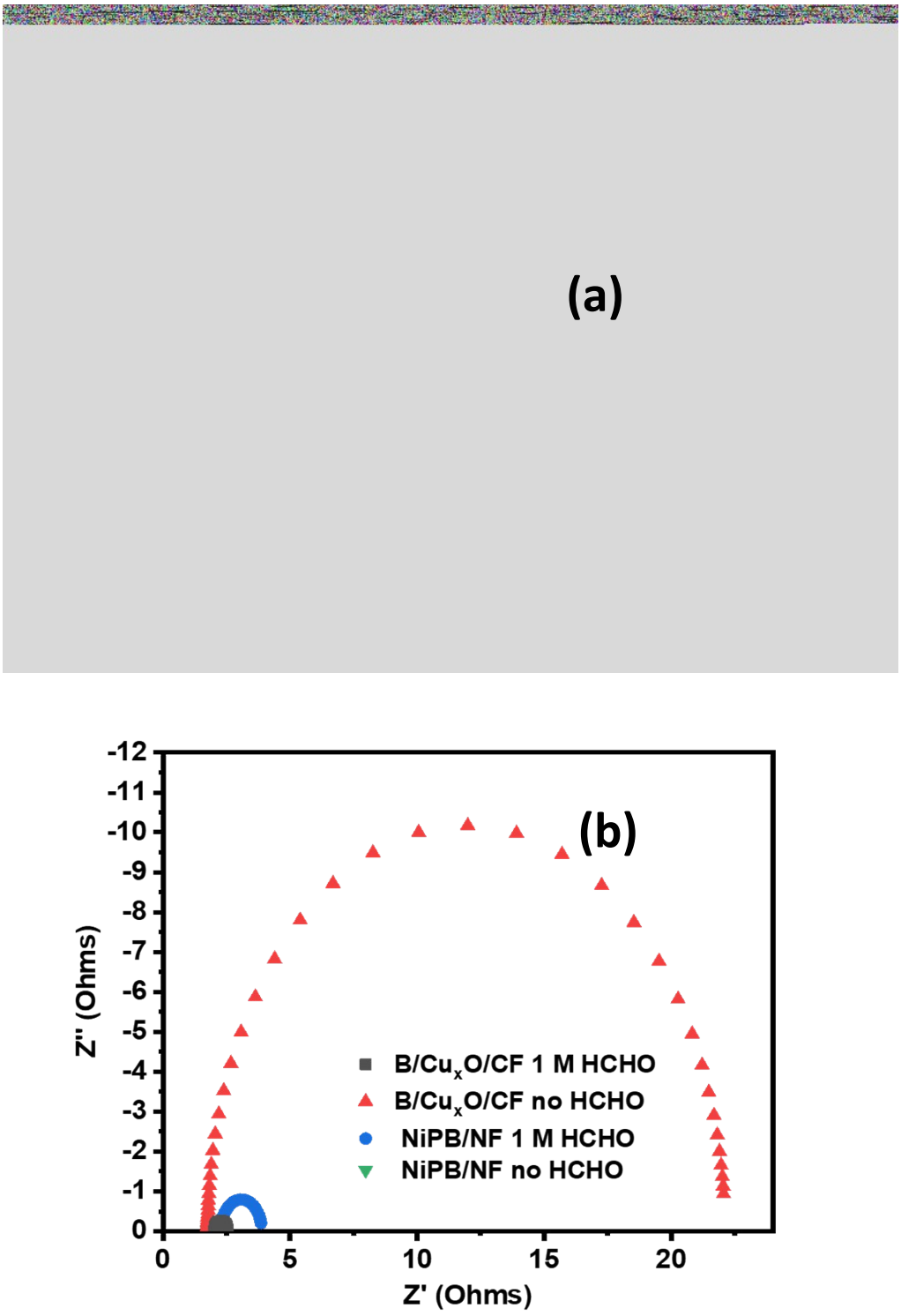

Fig. S17: (a) Nyquist plots of B, S, and P/CuxO/CF electrocatalysts for HER in 1 M HCHO + 1 M KOH. (b) Nyquist plots of B/Cu_xO/CF and NiPB/NF electrocatalysts for HER with and without the presence of HCHO.

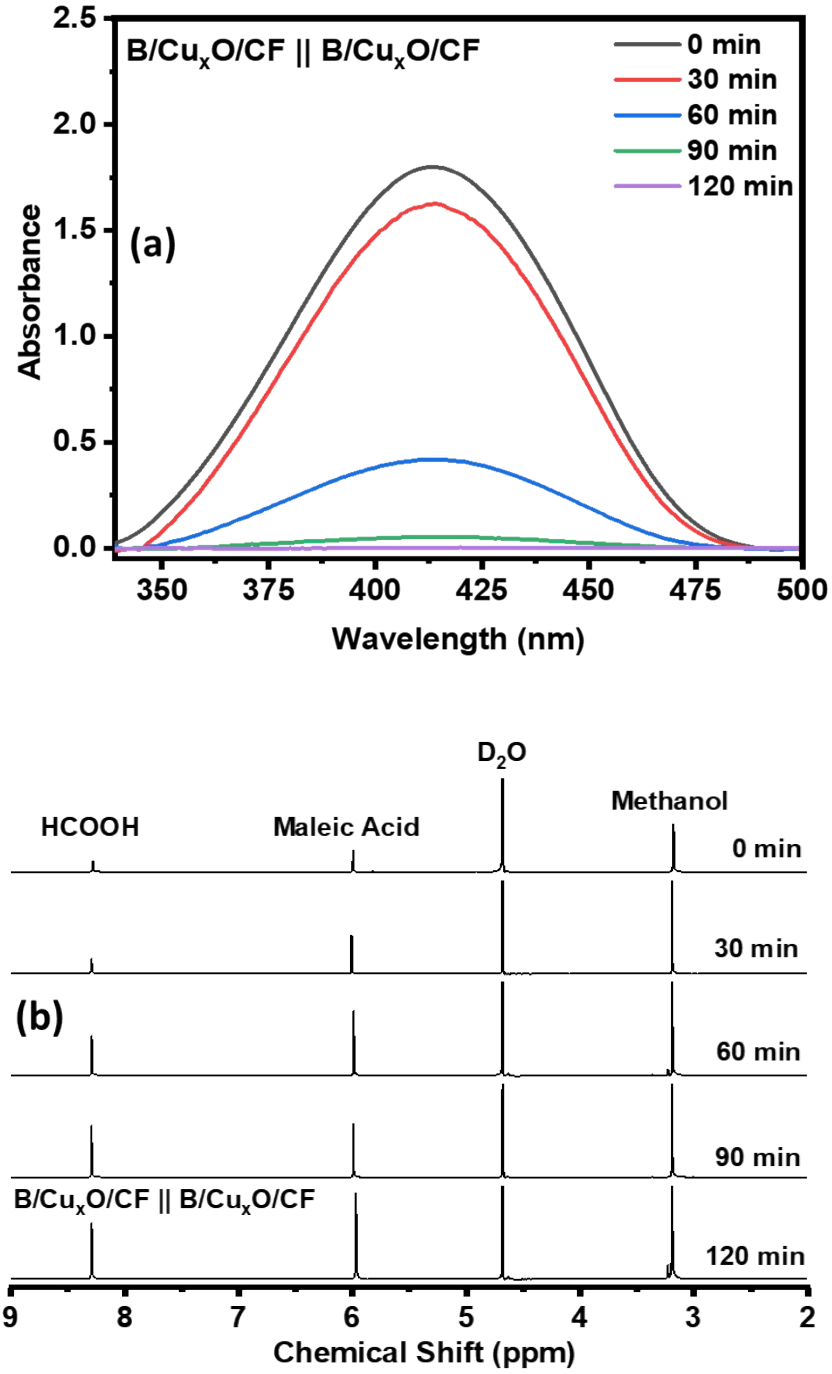

Fig. S18; (a) UV-Vis spectroscopy and (b) ^{1}H NMR spectroscopy at simultaneous periodic intervals during electrolysis test for B/Cu$_x$O/CF || B/Cu$_x$O/CF

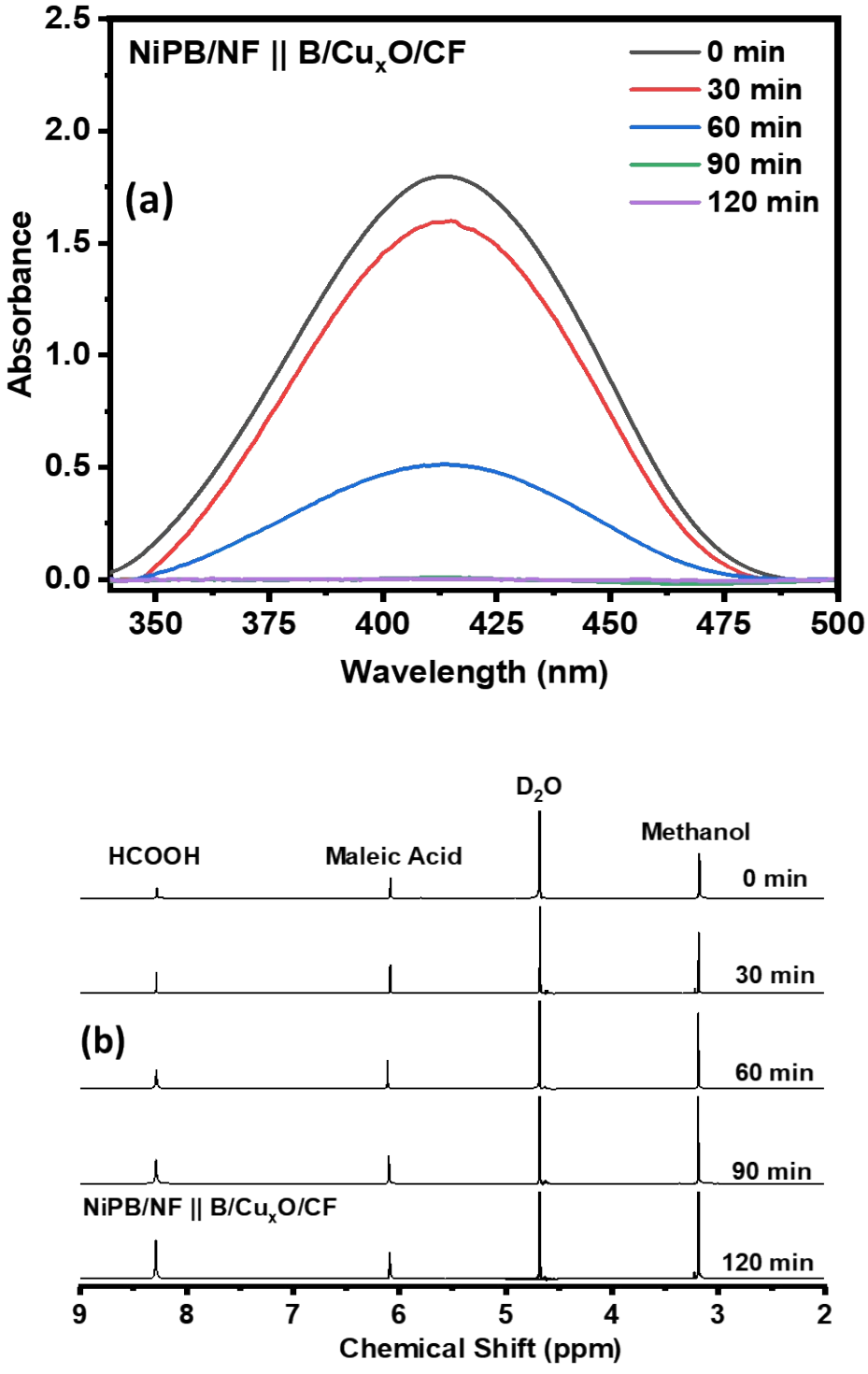

Fig. S19; (a) UV-Vis spectroscopy and (b) ^{1}H NMR spectroscopy at simultaneous periodic intervals during electrolysis test for NiPB/NF || B/Cu$_x$O/CF

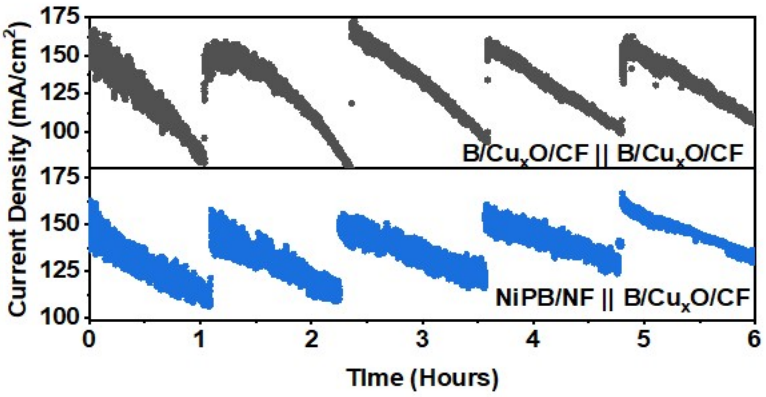

Fig. S20; Chronoamperommetry tests using a two electrode system (B/CuxO/CF|| B/CuxO /CF and NiPB/NF || B/CuxO /CF) with hourly periodic replenishment of HCHO.

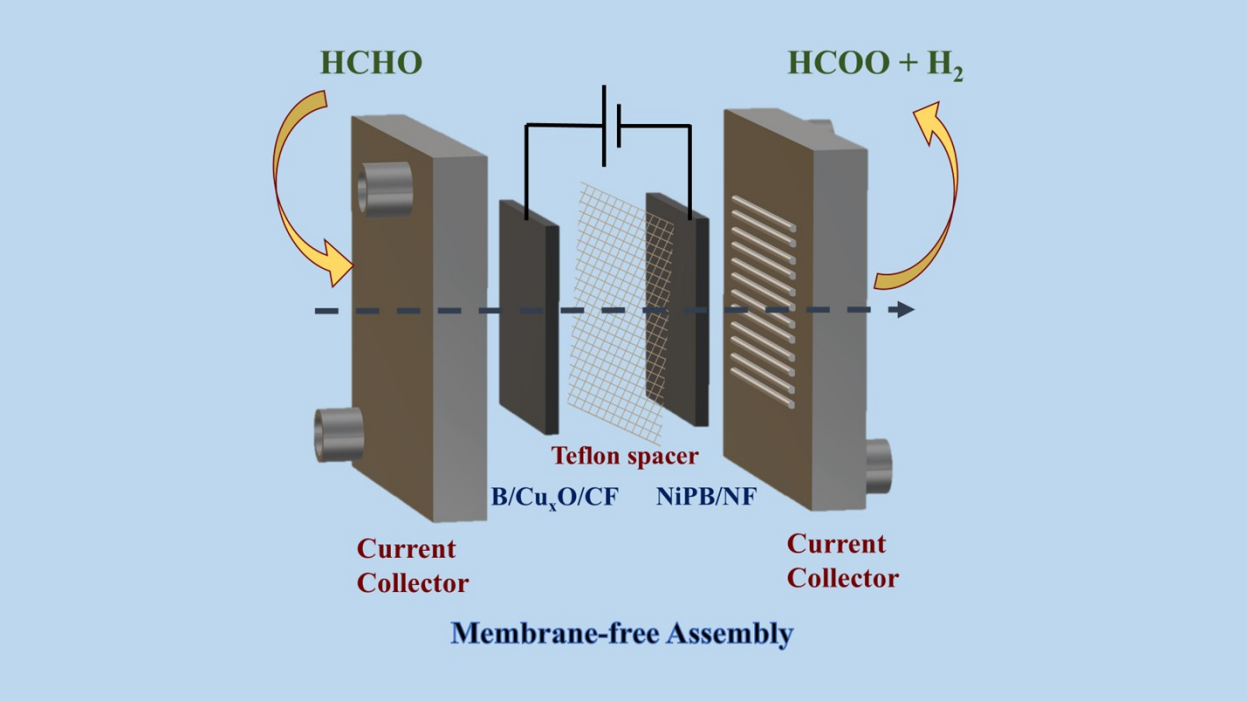

Fig. S21; Schematic of membrane-free assembly of asymmetric setup (NiPBNF || $B/Cu_xO/CF$)

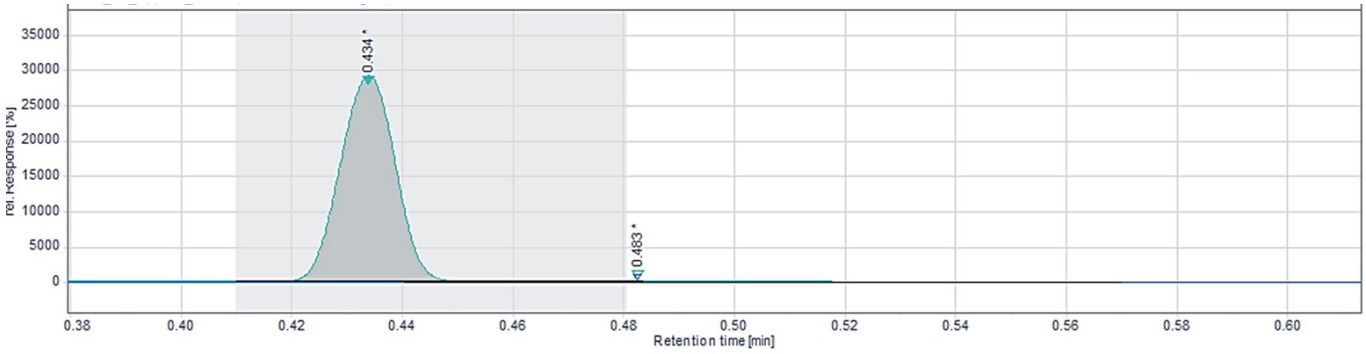

Fig S22; Gas chromatographic analysis of the product stream, for NiPB/NF || $B/Cu_xO/CF$ system

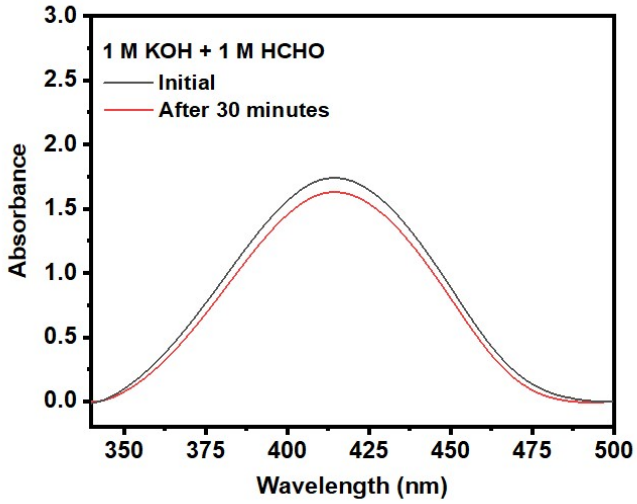

Fig. S23; UV- Vis spectra of spontaneous HCHO degradation over 30 min